

5.4 COMBINING NEW SATELLITE TOOLS AND MODELS TO EXAMINE THE ROLE OF MESOSCALE INTERACTIONS IN FORMATION AND INTENSIFICATION OF TROPICAL CYCLONES

Joanne Simpson¹
Goddard Space Flight Center/NASA, Greenbelt, Maryland
Elizabeth Ritchie,
Naval Postgraduate School, Monterey, California
W. Timothy Liu,
Jet Propulsion Laboratory/NASA, Pasadena, California
Christopher Velden,
University of Wisconsin, Madison, Wisconsin
Kurt Brueske,
Air Force Academy, Colorado Springs, Colorado
Harold Pierce,
Goddard Space Flight Center/NASA, Greenbelt, Maryland
Jeffrey Halverson,
University of Maryland, Baltimore County, Maryland

1. INTRODUCTION

This paper reports first results of an ongoing study of the formation (TD status) and early intensification of tropical cyclones using data from TRMM, AMSU and QuikSCAT, together with numerical model output, the NRL Web site (<http://www.nrlmry.navy.mil/>), and conventional data as available. Satellite tools such as these can examine tropical cyclones wherever they occur. We begin with Atlantic hurricanes because of a larger database and greater concern to the U.S. More than 50% of hurricanes originate from African waves often called "seedlings". We examined so far two African seedlings, both of which reached TD but only one intensified to a named hurricane (Floyd, 1999).

2. METEOROLOGICAL BACKGROUND

The formation of hurricanes has been a controversial problem, with few observations of mesoscale processes that might be important. It has been difficult to "catch" a hurricane forming with a fleet of instrumented aircraft. In the 1980's Ooyama (1982) and Schubert and Hack (1982) showed with models that the Rossby Radius of Deformation L_r had to be greatly decreased from its normal ~ 1500 km in the tropics for the latent heat released in convective systems to be retained locally, rather than being propagated away by gravity waves. This meant that the "background" vorticity had to be greatly increased above normal. High background vorticity is frequently found in monsoon troughs, making these the sites for development of most of the world's tropical cyclones (Greg Holland, personal communication). Our hypothesis is that there is an intermediate mesoscale step between high background vorticity and the formation of a Tropical Cyclone in many cases.

In 1997, Ritchie and Holland proposed that interaction of mesoscale vortices of dimension 200-500 km could be an important link in lowering the Rossby Radius, L_r . They had studied vortex models showing that when close together, two vortices may interact or "merge", with the weaker vortex giving up vorticity to the stronger and then shearing off in a pattern resembling a hurricane rainband.

Researchers (e.g. Menard and Fritsch, 1989) studying long-lived Mesoscale Convective Complexes (MCC's) over land discovered that the stratiform regions of such systems were an ideal environment for the growth of midlevel (4-8 km) elevation vortices on this scale. Miller and Fritsch (1991) and others found that these cloud systems lasted long enough (~ 24 hr) to allow the vortex to stabilize, so that when the stratiform anvil finally dispersed, the vortex remained coherent. Harr et al. (1996) documented that numerous similar systems in the tropical western Pacific also develop stable vortices on that scale. Because these mesoscale cloud systems permit developing vortices to remain stable with some reduction in L_r , they may provide important pre-conditions for the development of a tropical cyclone. Therefore we began testing a hypothesis concerning how these midlevel vortices might occasionally develop down to the surface with sufficient strength that increased fluxes of heat and moisture from the sea can begin the intensification cycle. The birth of one hurricane-force Tropical Cyclone, Oliver, was "caught" by two NASA aircraft off the east coast of Australia during TOGA COARE in 1993. The aircraft recorded the development, interaction and merger of two large Mesoscale Convective Systems (MCS's) that formed in association with midlevel vortices within a low-level monsoon cell (Simpson et al, 1997). A nearby island radar recorded the tracks of the two main mesoscale vortices by their rain echoes prior to and during the interaction of the mesoscale cloud

¹ Corresponding author address: Joanne Simpson,
Mail Code 912, Goddard Space Flight Center/NASA
Greenbelt, MD 20771;
email: simpson@agnes.gsfc.nasa.gov

systems. Results showed that the interaction both between the two midlevel vortices, and between the midlevel vortices and the low-level monsoon cell were important in the formation and development of a nascent eye in Oliver.

3. APPROACH

Our approach is to build a time sequence of three-dimensional mental pictures of each hurricane seedling studied. The goal is to understand and document the processes by which the system undergoes the observed changes between one and the next time interval. All observations available are used to build the time sequences. We used a global numerical model (NAVY NOGAPS) at 19 levels every 12 hr to describe the storms' environment and to tie the satellite observations together.

3.1 Use of Geosynchronous satellite data

The study benefited greatly from imagery from the GOES and Meteosat geosynchronous satellites. In particular, color-enhanced movie loops of the IR channel were used to depict early convective organization, overshooting towers preceding intensification, and detection of mid-level vortices. In addition, winds derived from the GOES and Meteosat multispectral imagery (Velden et al. 1998) and resultant vertical wind shear analyses (Gallina and Velden 2000) were useful in characterizing the shear environment during development.

3.2 New Satellite Technology, QuikScat, AMSU and TRMM and combinations available on the NRL Web Site

QuikSCAT has been the most revolutionary and most valuable for this study in that it provides winds at the sea surface as soon as the hurricane seedling moves off Africa. For this study, important QuikSCAT features are: its continuous 1,800-km swath that covers 93% of the global ocean in a single day; special products made with 12.5-km resolution for the hurricane seedling areas; and a wind range 3-30 m s⁻¹ (Liu, 2001). Rain contaminated data are not discarded in this investigation of early development.

AMSU-A is a satellite-borne passive microwave radiometer capable of monitoring the three-dimensional structure and evolution of tropical cyclone warm cores. Two-dimensional vertical cross-sections were developed in an effort to relate temporal variability in observed mid-to-upper tropospheric warming to convection within the tropical cyclone inner core region. Radiometric noise and error associated with the retrieved temperatures limited our ability to discern nascent warming to a lower threshold of approximately +/-2K.

From TRMM we use the passive microwave data mainly in connection with the data sets on the Naval Research Laboratory's Web Site. The site makes available visible and infrared GOES data, together

with the passive microwave (TMI) on TRMM and SSM/I, whenever overpasses with microwave sensors are made over tropical cyclones. A complete discussion of the Web Site products are found in Hawkins et al., 2001. Combinations of imagery are made with both the passive microwave sensors' high resolution channel (85 GHz) and with the 37 Hz channel of the TRMM TMI. The latter combination is made to enhance the low-level rainfall, which often develops with little ice scattering.

4. RESULTS AND DISCUSSION

Climatologically, more than half of Atlantic hurricanes originate in "seedlings" which move off Africa. QuikSCAT showed that for the 1999 season, the African monsoon trough frequently extended westward to 30° W and often reached as far north as 11-14° N. Calculated from the NAVY NOGAPS model, its "background vorticity" was frequently as large as 3 - 4 x 10⁻⁵ s⁻¹, the high value in the Australian monsoon trough at the birth of Oliver. It is clear that the background vorticity supplied by the extended monsoon trough over the ocean is likely to have reduced L_r adequately for vortices of 200-500 km to last long enough to merge and perhaps also for heat released by cumuli to be retained in the vortex. However, for African seedlings moving westward over the eastern Atlantic, life is not that easy.

Fig. 1 shows the Cape Verde sounding at 00 UTC on Sept. 4, 1999, when the pre-Floyd disturbance passed by to the south. Saturation in the lowest layer means low clouds, topped by a strong inversion and dry layer. The saturated layer from about 5 -7.5 km elevation indicates a middle cloud layer. Most noteworthy, if saturated air were forced upward through the inversion, it should be able to rise buoyantly since entrainment provides little drying above 400 mb.

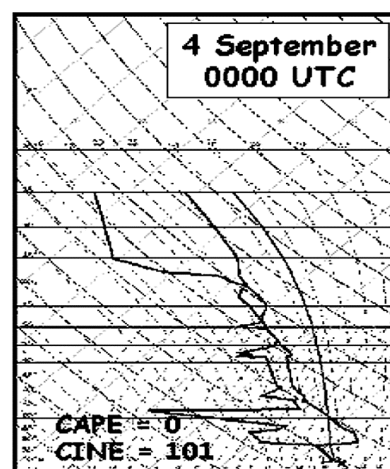


Fig. 1 Cape Verde Radiosonde for 00 UTC, Sept 4 1999. Typical for hurricane season.

4.1. The Birth and Early Life of Floyd 1999, September 2-5, 1999

Fig. 2 shows the track of Floyd plotted on underlying sea surface temperatures (SST's). The first circle indicates where the National Hurricane Center declared Floyd a TD, half way across the Atlantic on Sept 7. The x's follow the center of the vortex observed on QuikSCAT, combined with the infrared movie. The pre-Floyd disturbance moved off Africa on 2 Sept with a weak surface vortex signature in the scatterometer data and moderate convection organized into an MCS (area ~ 10,000 km²) to the northeast of the center. It took another 5 days of struggling before Floyd was declared a TD.

During the first two days there was unfavorable wind shear greater than 7 ms⁻¹ between the lower and upper air layers, which fell below 5 ms⁻¹ on Sept 4 and thereafter. Also the SST's off Africa were marginal for development, less than about 27°C. However, the NOGAPS model showed the vortex was quite deep, extending down from 500 mb, with associated surface circulation of 4-6 ms⁻¹ indicated by the scatterometer. Some convergence and low-level inflow was associated with the surface vortex so that the forcing was probably enough for a few cumulonimbus clouds to penetrate the inversion and form anvils. The IR image for 1925 UTC Sept 2 (not shown) had some

towers up to 12-14 km, but the movie shows they disappeared in 12 hr or less. The rotational winds of the surface vortex seen in the scatterometer data weakened only slightly between Sep 3 and 4, although little convection developed close to the vortex center (black dot on Fig. 3). However, Figs 3a-d show an MCS that developed or redeveloped each day in the same relative location north of the vortex center. The anvils were large and long lasting enough to sustain the 200-500 km scale vortices. These could be the cause of the sustained, or slightly increased, strength of the surface vortex, especially if the vortex tilted north with height.

By Sept 5, there were two detectable midlevel vortices (Fig. 3d) in the IR movie. One was clearly associated with the MCS to the north of the surface circulation center and the other was a midlevel reflection of the surface circulation tracked by QuikSCAT. The two midlevel vortex centers merged during the 5th of Sept, intensifying the surface vortex winds by 2- 4 ms⁻¹. Fig 2 shows that pre-Floyd briefly crossed an ocean area with SST of only about 26°C during this merging time on Sept 5th. By late on Sept. 5 pre-Floyd again moved over increasing SST's. A pool of warmer θ_e air started appearing to the north of the system, partially built up by the swirling flow around the east and north side of the vortex itself.

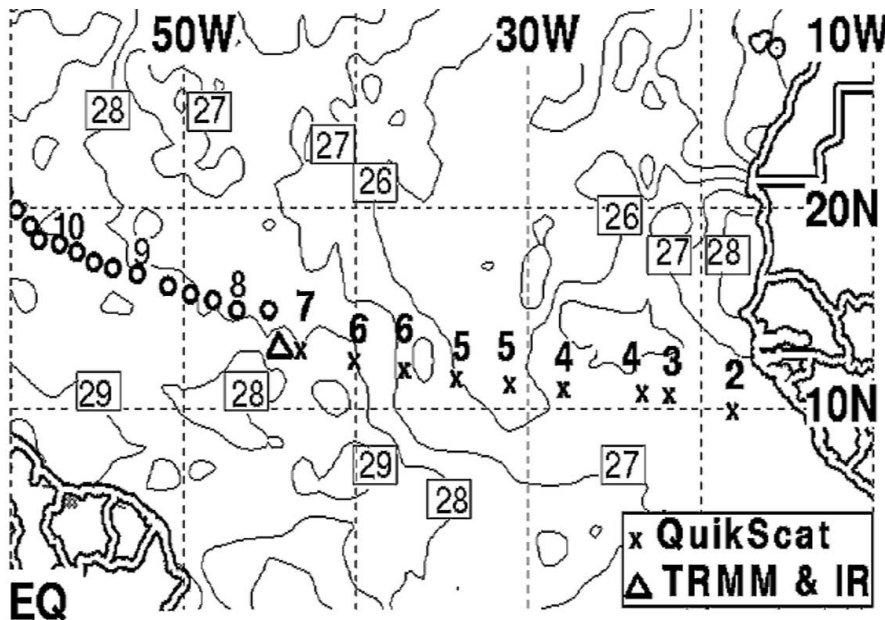


Fig. 2 Track of Floyd 1999 on background of Sea Surface Temperatures

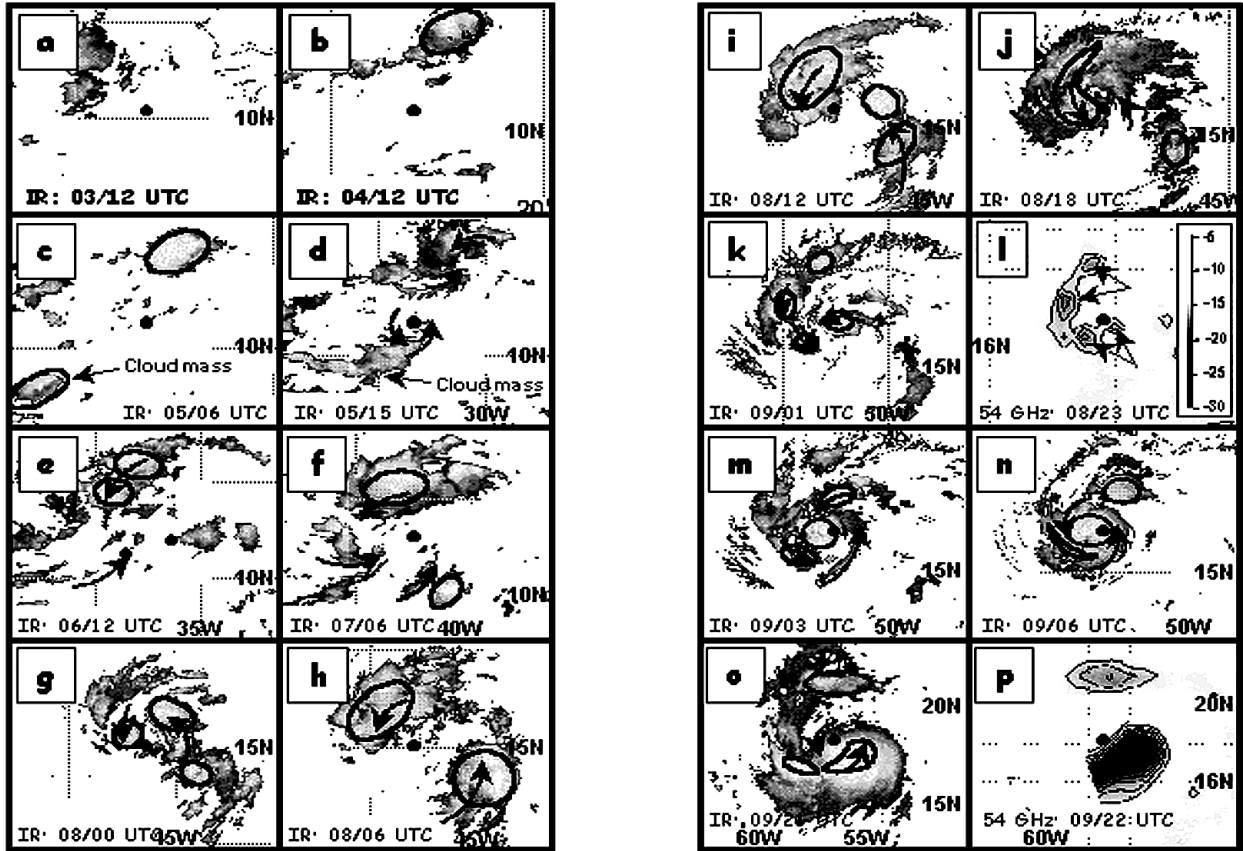


Fig. 3 Sequence of METEOSAT IR and AMSU-A 53.6 GHz images for early Floyd. Times, image type, on each panel. The thin black outlines indicate inferred vortices and black arrows show where cloud rotation was observed in the IR movies

4.2 Pre-Floyd's intensified convection and start of low-level incursion of high θ_e air, Sept. 6-9, 1999

By late on Sept. 6, pre-Floyd was moving over 28°C water. The scatterometer image shows two surface vortices merging. Taking into account the 1.3° northward jump on the track from 1950 UTC on the 5th to 0800 UTC on the 7th, events enacted a perfect merging scenario of these two vortices. By 0800 UTC on Sept.7, the QuikSCAT image showed a single vortex with an area of increased and highly sheared winds on its eastern edge. This is a perfect match with Ritchie's merging vortex model, a classic picture of a sheared losing vortex merged into the victor.

4.3. How Floyd Got the Hurricane Engine Started

The story of hurricane development is the story of successful interaction of many different scales of motion. The new technology which became available in the late 1990's (TRMM, AMSU, and QuikSCAT) has enabled us to observe and link together several interactions that previously had only fragmentary data to interpret. The NOGAPS model relates the vortex center to the field of θ_e . On Sept. 7, the vortex center was far from the high (above 252°K) θ_e air, while on

Sept. 8, the center was on the edge of the high θ_e pool. On Sept. 9, the pool of 360°K air was in and to the north of the center, while 24 hours later, the highest energy air was found in the core of the storm. However, mesoscale processes are again required, both to build the bomb and to set it off.

By Sept. 6, the pre-Floyd circulation had moved over sea surface temperatures of higher than 28°C , which raised the θ_e of the inflowing air by increasing fluxes from the ocean to the lower air. This warming, moistening and destabilization of the air caused convection to be much more active, with multiple developments within about 4° of the center of the surface circulation (Figs 3 e, f). As existing mesoscale systems dissipated, new ones were already developing. The associated vortex mergers into the primary circulation resulted in an intensification of the surface swirling winds to greater than 8 ms^{-1} by late on the 7th of Sept, when Floyd was declared a TD by the National Hurricane Center. On the 8th, two substantial mesoscale systems began to develop, one to the east-southeast and one to the west-northwest of the center of the circulation. The two mesoscale convective systems rotated and merged over an 18-hr period (Figs 3,f-j) in a manner analogous to those for TC Oliver 1993. There was a hint of a nascent eye wall at 1800 UTC on 8 Sept. (Fig. 3 i) as the western

clouds wrapped around the center of circulation in a hook pattern also similar to that of Tropical Cyclone Oliver. In contrast to Oliver, however, another two days passed until Floyd intensified to hurricane strength. There was no marked drop in central pressure until mid-day on Sept. 9.

Fig. 4 shows storm relative winds, calculated from QuikSCAT data, on Sept. 8th and 9th. As late as Sept 8th at 2155 UTC when Floyd was already a Tropical Storm, the high θ_e air moves around the periphery of the storm (Fig. 4 top). On Sept. 9, Fig 4 (bottom) shows a region about 100 km across getting in to the core on the rear quadrants (from the east), setting the stage for the convective burst discussed later. On QuikSCAT the winds are now above 8 ms^{-1} out to a radius from center of more than 220 km and $6\text{-}8 \text{ ms}^{-1}$ twice that far out. This means the ocean-air fluxes are already increased, causing the convection to be much more active within 400 km of the surface circulation center.

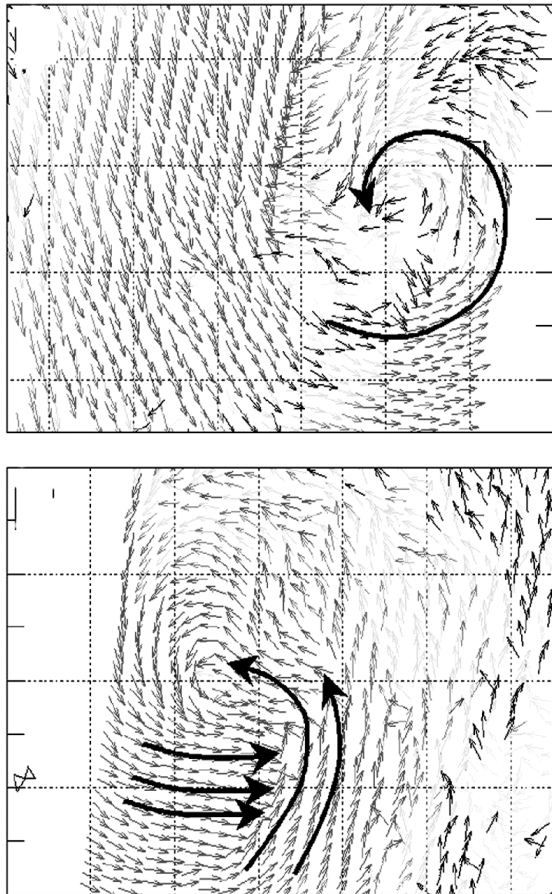


Fig. 4 QuikSCAT images for 2155 UTC Sept 8, 1999 (top) and 2130 UTC on Sept 9 (bottom)

4.4 Floyd's First Two Convective Bursts

Floyd's rapid intensification period commenced early on 9 Sept. with the sudden eruption of intense hot

towers in the form of convective bursts (Fig. 5). Two bursts were identified through inspection of combined

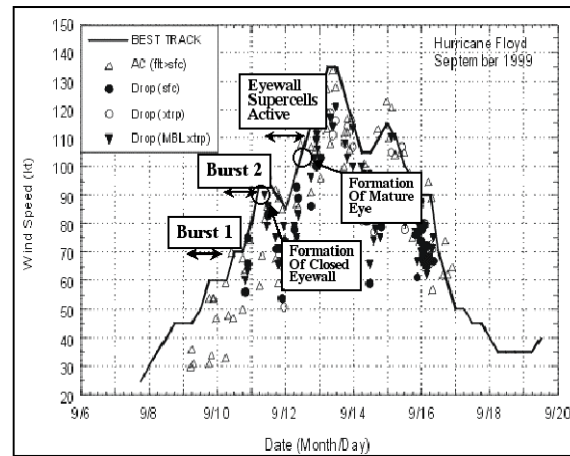


Fig. 5 Floyd's convective bursts, on windspeed and other events plotted against date/time.

GOES infrared and passive microwave imagery. We hypothesize that these convective bursts were essential for warm core development, the rapid deepening, and eye formation in Floyd, and they provide a crucial link between the forcing (i.e. convergence due to low-level wind surges) and vortex-scale intensification.

Figure 5 reveals that each burst was active for approximately 24 hours and followed in close succession during the period of most rapid vortex spin-up. Both of these bursts featured a cold, circular cirrostratus shield that expanded to 400-500 km diameter during maximum extent, with repeated eruption of overshooting hot towers occurring within the center of the cloudy mass. Minimum cloud top temperatures in the tallest overshoots approached $-85 \text{ }^\circ\text{C}$. Formation of a closed low-level eyewall occurred during the latter stage of Burst 2, when the storm's maximum sustained winds approached 50 ms^{-1} on 11 September.

4.5 Floyd's Warm Core Development

One of the most noteworthy aspects of Floyd's development was the length of time it took to develop a warm core in the upper levels. An upper-level warm core is necessary to support both the low central pressure and the strong winds at the surface. Despite the continued development of convection particularly throughout the period 6-8 September, it wasn't until the early hours of September 9 when the towers in the first convective burst carried the necessary high energy air to high levels that a warm core was finally observed to begin developing in AMSU-A data. At 2300 UTC on September 8, Floyd showed no significant warm core (not shown). By 1200 UTC on the 9th, after the first major hot tower eruption, a slight increase in the brightness temperature, which equates to $\sim 1^\circ\text{C}$ of real warming was observed. A

corresponding increase of surface winds then resulted in an increase in the ocean fluxes and thus the energy of the surface air that ascended in the second burst, so that by late on September 10th, the warm core had increased again to about a 2 °C equivalent maximum temperature anomaly (not shown). At that time, maximum winds had exceeded 36 m s⁻¹ and a complete nascent eye wall exists. Finally by late on the 11th September, at the end of the second burst, warm core anomalies of about 7°C at 250 mb and 6.2°C at 150 mb were observed in the AMSU data. When computed hydrostatically this warm “core” would support a 31 mb reduction in the surface pressure relative to September 8. This is consistent with NHC’s pressure data of 1000 mb on September 8 and 967 mb by the end of September 11. Figure 5 shows Floyd’s intensification through September 13, and subsequent weakening, which is beyond the scope of this Chapter.

The explanation for the slow development of the warm core is found by examining the NOGAPS sequence of θ_e near the surface and in the mid-troposphere. A relationship found in the 1960’s between central pressure fall and increase in θ_e in the ascending undilute eyewall clouds, shows that the rising air in the eyewall clouds must increase its energy in terms of θ_e by 12 ° relative to the environment. In Floyd, this would mean a change from about 354K to about 366K. By late on September 11, the boundary layer θ_e was 380K, which sounds great. However, much dilution must have occurred in the towers of the convective bursts, because the mid-level θ_e was still only 348K. Since a mixture as large as 40 per cent of 348K air with 60 per cent rising 380K air from the low levels gives the required 366K for the pressure fall, our results are reasonable. The midlevel air encountered remained very dry and energy is being lost to moisten it, accounting for the very slow development of the Floyd warm core. For more on AMSU, see Brueske et al., 2001.

4.6 TD2, June 22-26, 2000

Experienced forecasters would not expect African seedlings to become hurricanes in June, owing to cool ocean waters and unfavorable soundings. However, we examined a vortex stronger than the pre-Floyd vortex when it left Africa, which came close to being named. It also traveled as far westward across the Atlantic Ocean as pre-Floyd (Fig. 6 compared with Fig. 2).

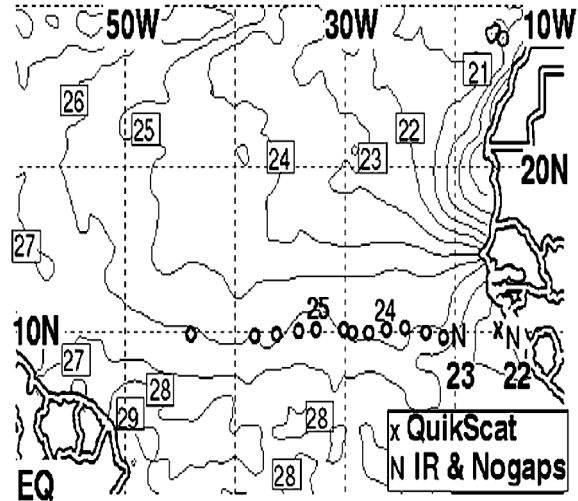


Fig. 6 Track of TD2, June 22-26, 2000 on background of Sea Surface Temperatures

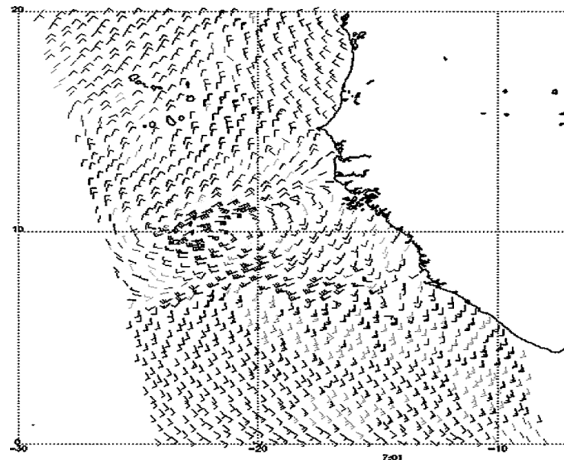


Fig. 7 QuikSCAT overlapping swaths at 0700 UTC June 23, 2000. Wind barbs in knots.

During the period 21-23 June 2000, the large-scale dynamic environment off the west coast of Africa appeared favorable for development. The vorticity in the monsoon trough zone was weaker than that for Floyd at the surface. However, it was much stronger at 700 mb, adequate to permit 200-500 km mesoscale vortices to persist. The ambient vertical wind shear was less than 6 ms⁻¹. The disturbance moving off Africa appeared deep, extending downwards from 500 mb in NOGAPS analyses, with an associated surface circulation of about 10 ms⁻¹. There was a confluence region ahead of the disturbance as shown in a later scatterometer image. The convergence in this region was as large as $20 \times 10^{-6} \text{ s}^{-1}$ for 23 June. A maximum value of $10 \times 10^{-6} \text{ s}^{-1}$ persisted over a large region throughout the disturbance (NOGAPS). The convergence was of great importance to the events that followed.

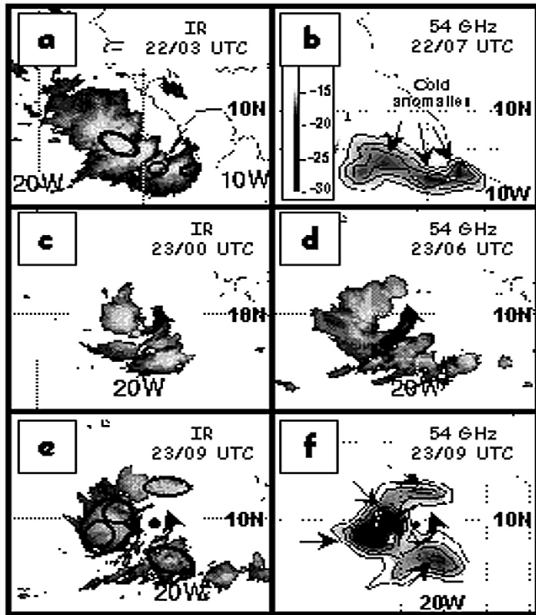
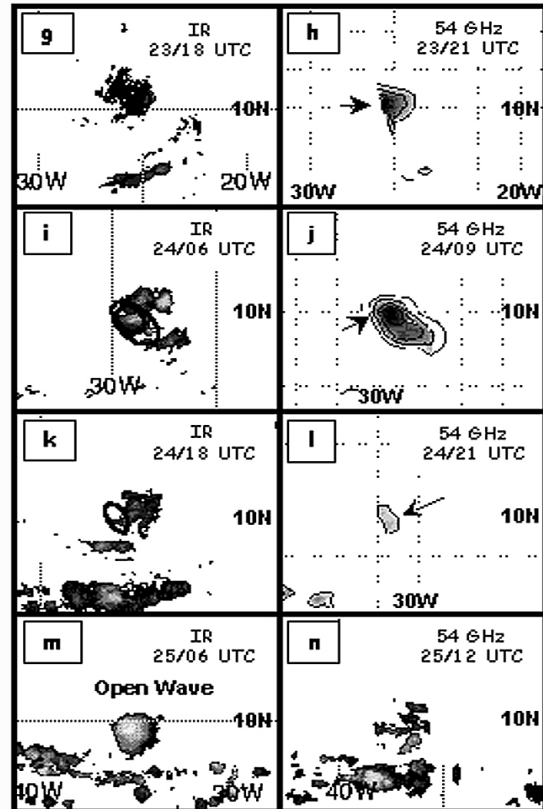


Fig. 8 Sequence of METEOSAT IR and AMSU-A 53.6 GHz images. Time and type of image are indicated on each panel. The thin black outlines indicate inferred vortices and black arrows show where cloud rotation was observed in the IR movies



Another important feature was a bulge of high sea surface temperatures (SST's) above 28°C just off the coast, as shown in Fig 6. This warm ocean area caused the low-level air to have unusually warm energy content, with a surface θ_e higher than 350 K . Warning notes are struck by the low mid-level θ_e of about 335° K , and particularly by the stable, dry atmospheric sounding at Dakar (not shown). It has a stronger inversion, no saturated layers, and a much drier air mass than does Fig 1. Thus a stronger "push" or upward forcing is required for penetrative clouds, and much more moistening of the environment would be necessary to "ripen" conditions enough for a convective burst.

The warm, moist low-level air, however, was given enough upward "push" by the convergence ahead of the seedling to create four or five convective towers simultaneously which reached higher than about 15 km as seen in the IR at 0845 UTC on 22 June. High towers became less numerous after that time. The last high tower was observed at 2250 UTC June 22. No cloud tops colder than 240°K , or about 13 km height were observed thereafter, with most clouds topping below 9 km . The main explanation for the diminishing strength and penetration of cumulonimbus towers is the decreasing energy θ_e of the low-level air as the TD moves westward over the cooler ocean typical for June in this region. By 2250 UTC on the 22nd, the θ_e of the underlying air has decreased by 8°K . Also the dryness of the midlevel air in June dilutes cloud towers, killing their

buoyancy. There was no evidence in the AMSU data for warming aloft as a result of convection associated with TD2.

Although convective towers failed to reach above $12\text{-}13\text{ km}$ after about 2250 on June 22, the TD2 vortex most closely approached hurricane wind speed and structure about 9 hr later, on the early morning of June 23 (Fig. 7). Fig. 8 shows this strengthening and organization was produced by the merging of midlevel vortices.

As TD2 first moved off Africa on June 22 (Fig 8a,b) convergence of high low-level θ_e air resulted in the development of several mesoscale convective systems with cold IR tops asymmetrically organized around the east and south of the center of the disturbance. The passive microwave images (not shown) reveal that the rain showers were more symmetrically distributed. However, the vertical wind shear increased during the day to more than 6 ms^{-1} from the east-southeast. As a consequence, the clouds became sheared and moved to the southwest of the circulation center. Although three vortices were identified with the aid of AMSU imagery, no merger was indicated in the cloud patterns.

By 2100 UTC on June 22, the wind shear had weakened, and the first of several new mesoscale convective systems developed just to the south of the surface circulation. As a result of lower θ_e in this region, there were fewer convective cells, and the associated stratiform anvils were smaller in extent (Fig 8c vs. Fig 8a). However, during the day of June

23, scatterometer imagery (Fig. 7) shows that TD 2 reached its peak winds close to 25 ms^{-1} . Moreover, combining the 85 GHz channels of the passive microwave instrument on TRMM (not shown) a configuration resembling a nearly closed hurricane eye appeared.

The mesoscale vortex interactions which produced this event are shown in Figs 8 (e-f). QuikSCAT imagery (Fig. 7) suggested that this vortex had winds above those required for a named storm. It also showed considerably strong rotation in the cloud systems. Forecasters resisted the pressure to name it because the high winds did not last for a 6-hr forecast interval. As the TD2 disturbance moved west of about 25° W late on June 23, the sea surface temperatures decreased to less than 26° C (Fig. 6) and both the low- and mid-level θ_e ahead of the disturbance had decreased. Some convection continued for more than 24 hours, but the tops were shallower ($\sim 12 \text{ km}$), Figs 8 l-m show the gradual decay. On June 25, TD2 had deteriorated to an open wave, after travelling more than 2500 km westward.

5.0 CONCLUDING REMARKS

The most important conclusion is that the new satellite instruments in combination have enabled us to show that mesoscale vortex interactions are extremely important in the development of hurricane seedlings originating in Africa. Vortex mergers enabled the Floyd seedling to travel far enough westward and live long enough to obtain an environment suitable for intensification.

For TD2 2000 thermodynamic conditions were unfavorable for intensification. But the system was able, by vortex merger, to reach near storm strength surface winds. Its prolonged life did not require intense deep convection. The main role that convection played was to provide the stratiform anvils making conditions suitable for the mesoscale midlevel vortices to last and to merge. This importance of dynamics in the early stages and relative unimportance of deep convection is quite contrary to most of the earlier ideas of Tropical Cyclone genesis, which usually start by discussing clusters of deep convective clouds.

6.0 ACKNOWLEDGMENTS

The authors are grateful to J. Hawkins and colleagues of the Naval Research Laboratory for providing easy access to IR and passive microwave satellite imagery and much additional help. We are grateful to Dr. Scott Tyo for providing his expertise on image enhancement techniques. The work was supported by the NASA TRMM program, under Dr. Ramesh Kakar, NASA Headquarters Program Scientist and by the Office of Naval Research Marine Meteorology Program, under Dr. Robert Abbey, by the U.S. Air Force and its Department of Physics.

We are also grateful to Stacy Stewart and Miles Lawrence of the National Hurricane Center for much

help and information and to G. Heymsfield and R.H. Simpson for many helpful discussions.

7.0 REFERENCES

- Brueske, K.B. and C.S. Velden 2001: Satellite-based TC intensity estimation using the NOAA series AMSU. Conditionally accepted in *Mon. Wea. Rev.*
- Gallina, G. and C.S. Velden, 2000: A quantitative look at the relationship between environmental vertical wind shear and TC intensity change utilizing enhanced satellite derived wind information. 24th Conf. Hurr. and Trop. Meteor., Ft. Lauderdale, FL, 256-257.
- Gray, W. M., 1975: Tropical Cyclone genesis. Dep't. of Atmos. Sci. Paper No. 234, Colo. State Univ., Ft. Collins, CO, 121 pp.
- Harr, P. A., M. S. Kalafsky, and R. L. Elsberry, 1996: Environmental conditions prior to formation of a midlevel tropical cyclone during TCM-93. *Mon. Wea. Rev.*, **124**, 1693-1710.
- Hawkins, J., T. F. Lee, J. Turk, C. Sampson, J. Kent and K. Richardson, 2001: Real time internet distribution of satellite products for Tropical Cyclone reconnaissance. *Bull. Amer. Met. Soc.*, **82**, 567-578.
- Liu, W. T., 2001: Wind over troubled water, *Backscatter*, **12**, 10-14.
- Menard, R. D., and J. M. Fritsch, 1989: A mesoscale convective complex-generated inertially stable warm core vortex. *Mon. Wea. Rev.*, **117**, 1237-1261.
- Miller, D. and J. M. Fritsch, 1991: Mesoscale convective complexes in the western pacific region. *Mon Wea. Rev.*, **119**, 2978-2992.
- Ooyama, K., V., 1982: Conceptual evolution of the theory and modeling of the tropical cyclone. *J. Met. Soc. Japan*, **60**, 369-380.
- Ritchie, E. A. and G. J. Holland, 1997: Scale interactions during the formation of Typhoon Irving. *Mon. Wea. Rev.*, **125**, 1377-1396.
- Schubert, W.H., J.J. Hack, P.L. Silvia Dias and S.R. Fulton, 1980: Geostrophic adjustment in an axisymmetric vortex. *J. Atmos. Sci.*, **37**, 1464-1484.
- Simpson, J., E. A. Ritchie, G. J. Holland, J. Halverson, and S. Stewart, 1997: Mesoscale interactions in tropical cyclone genesis. *Mon. Wea. Rev.*, **125**, 2643-2661.
- Velden, C.S., T.L. Olander and S. Wanzong, 1998: The impact of multispectral GOES-8 wind information on Atlantic tropical cyclone track forecasts in 1995. Part 1: Data set, methodology, description, and case analysis. *Mon. Wea. Rev.*, **126**, 1202-1218.